

On the Value of Labeled Data and Symbolic Methods for Hidden Neuron Activation Analysis

Abhilekha Dalal¹, Rushrukh Rayan¹, Adrita Barua¹, Eugene Y. Vasserman¹,
Md Kamruzzaman Sarker², and Pascal Hitzler¹

¹ Kansas State University, Manhattan, KS, USA

² Bowie State University, Prince George's County, MD, USA

Abstract. A major challenge in Explainable AI is in correctly interpreting activations of hidden neurons: accurate interpretations would help answer the question of what a deep learning system internally detects as relevant in the input, demystifying the otherwise black-box nature of deep learning systems. The state of the art indicates that hidden node activations can, in some cases, be interpretable in a way that makes sense to humans, but systematic automated methods that would be able to hypothesize and verify interpretations of hidden neuron activations are underexplored. This is particularly the case for approaches that can both draw explanations from substantial background knowledge, and that are based on inherently explainable (symbolic) methods.

In this paper, we introduce a novel model-agnostic post-hoc Explainable AI method demonstrating that it provides meaningful interpretations. Our approach is based on using a Wikipedia-derived concept hierarchy with approximately 2 million classes as background knowledge, and utilizes OWL-reasoning-based Concept Induction for explanation generation. Additionally, we explore and compare the capabilities of off-the-shelf pre-trained multimodal-based explainable methods.

Our results indicate that our approach can automatically attach meaningful class expressions as explanations to individual neurons in the dense layer of a Convolutional Neural Network. Evaluation through statistical analysis and degree of concept activation in the hidden layer show that our method provides a competitive edge in both quantitative and qualitative aspects compared to prior work.

Keywords: Explainable AI · Concept Induction · Convolutional Neural Network · Knowledge Graph · Large Language Model · Multimodal Model.

1 Introduction

The explainability of the decision-making process within Deep Learning solutions is a crucial element for their integration into safety-critical systems. Robust Explainable AI techniques not only provide insights into the operations of hidden layer neurons, which significantly impact model outcomes, but also facilitate

network debugging, causal factor analysis, and adjustments to data and network architecture, among other areas, to enhance model performance.

Standard assessments of deep learning performance consist of statistical evaluation, but do not seem sufficient as they cannot provide reasons or explanations for particular system behaviors [9]. While there has been significant progress in the Explainable AI domain (see Section 2), the current state of the art is mostly restricted to explanation analyses based on a relatively small number of predefined explanation categories. This is problematic from a principled perspective, as it relies on the assumption that explanation categories pre-selected by humans would be viable explanation categories for deep learning systems – an as-yet unfounded conjecture. Other approaches rely on deep learning itself, e.g., Large Language Models, to produce explanations [27] – which means that the explanation generation method in turn is yet another black box. Other state of the art explanation systems rely on modified deep learning architectures, usually leading to a decrease in system performance compared to unmodified systems [47]. The ideal approach would exhibit strong explanation capabilities, would be self-explainable, and can take a very large pool of possible explanation categories into consideration.

Many Explainable AI techniques rely on intricate low-level data features projected into a higher-dimensional space in their explanations, limiting their accessibility to users with domain expertise [31,23,36]. Some of these methods have shown vulnerability to adversarial tampering, wherein altering attributed features does not prompt a change in the model’s decision [3,41,38]. Conversely, there are high-level concept-based Explainable AI approaches, where manually selected concepts are measured for their correlation with model outcomes. However, a significant question remains unanswered: whether the limited set of chosen concepts can offer a comprehensive understanding of the model’s decision-making process. The absence of a systematic approach to consider a wide range of potential concepts that may influence the model appears to be the bottleneck. In some techniques [27], a list of frequently occurring English words has been utilized to represent a broad concept pool, which may suffice for general applications but lacks granularity for specialized fields like gene studies or medical diagnoses, as the curation of the concept pool does not provide low-level control over defining natural relationships among concepts.

Our approach is motivated by several key principles: firstly, explanations should be understandable to end-users without requiring intimate familiarity with deep learning models. Secondly, there should be a systematic organization of human-understandable concepts with well-defined relationships among them. The extraction of relevant concepts for explaining a deep learning model’s decision-making process from this defined concept pool should be automatic, thus eliminating the bottleneck of manual curation prone to confirmation bias. Another significant goal is that the explanation generation technique itself should be inherently interpretable, avoiding the use of black-box methods.

Concretely, we address herein the following common shortcomings in the state of the art.

- i. Concepts should not be hand-picked in light of completeness.
- ii. Concept extraction methods should be inherently explainable.
- iii. Concepts should be understandable to the end-users without requiring deep learning expertise.
- iv. Label Hypothesis concept pool should include meaningful relationships between concepts, that are made use of by the explanation approach.

We address these points by using *Concept Induction* as core mechanism, which is based on formal logic reasoning (in the Web Ontology Language OWL) and has originally been developed for Semantic Web applications [21]. The benefits of our approach are: (a) it can be used on unmodified and pre-trained deep learning architectures, (b) it assigns explanation categories (i.e., class labels expressed in OWL) to hidden neurons such that images related to these labels activate the corresponding neuron with high probability, (c) it is inherently self-explanatory as it is based on deductive reasoning, and (d) it can construct labels from a very large pool of interconnected categories.

We hypothesize that a background knowledge with the skeleton of an ontology coupled with the inherently explainable deductive reasoning (Concept Induction) should be capable of generating meaningful explanations for the deep learning model we wish to explain.

To show that our approach can indeed provide meaningful explanations for hidden neuron activation, we instantiate it with a Convolutional Neural Network (CNN) architecture for image scene classification (trained on the ADE20K dataset [50]) and a class hierarchy (i.e., a simple ontology) of approx. $2 \cdot 10^6$ classes derived from Wikipedia as the pool of explanation categories [34].³ Our findings suggest that our method performs competitively, as assessed through Concept Activation analysis, which measures the relevance of concepts within the hidden layer activation space, and through statistical evaluation. When compared to other techniques such as CLIP-Dissect [27], a pre-trained multimodal Explainable AI model, and GPT-4 [1], an off-the-shelf Large Language Model, our approach demonstrates both strong quantitative and qualitative performance.

Core contributions of the paper are as follows.

1. A novel zero-shot model-agnostic Explainable AI method that explains existing pre-trained deep learning models through high-level human understandable concepts, utilizing symbolic reasoning over an ontology (or Knowledge Graph schema) as the source of explanation, which achieves state-of-the-art performance and is explainable by its nature.
2. A method to automatically extract *relevant concepts* through Concept Induction for any concept-based Explainable AI method, eliminating the need for manual selection of Label Hypothesis concepts.
3. An in-depth comparison of explanation sources using statistical analysis for the hidden neuron perspective and Concept Activation analysis for the hid-

³ Source code, input data, raw result files, and parameter settings for replication are available online at <https://anonymous.4open.science/r/xai-using-wikidataAndEcii-91D9/>

den layer perspective of our approach, a pre-trained multimodal Explainable AI method (CLIP-Dissect [27]), and a Large Language Model (GPT-4 [1]).

The rest of the paper is organized as follows: in Section 2, the recent approaches in Explainable AI domain are highlighted. In Section 3, the detailed overview of the our approach along with the protocol followed to adapt CLIP-Dissect and GPT-4 for the use-case is presented. In addition to that, the description of the statistical evaluation protocol and Concept Activation analysis are presented. In Section 4, we highlight the key findings of our method and the comparative analysis with other approaches. Section 5 presents the key observations and trade-offs of our approach, CLIP-Dissect, and GPT-4. Finally, Section 6 outlines the drawbacks and future scope of our study.

2 Related Work

Explaining (interpreting, understanding, justifying) automated AI decisions has been explored from the early 1970s. With the recent advances in deep learning [20], its wide usage in nearly every field, and its opaque nature make explainable AI more important than ever, and there are multiple ongoing efforts to demystify deep learning [13,2,25]. Existing explainable methods can be categorized based on input data (feature) understanding, e.g., feature summarizing [37,31], or based on the model’s internal unit representation, e.g., node summarizing [49,5]. Those methods can be further categorized as model-specific [37] or model-agnostic [31]. Another kind of approach relies on human interpretation of explanatory data returned, such as counterfactual questions [44].

Model-agnostic feature attribution techniques, exemplified by LIME [31] and SHAP [23], aim to explain model predictions by measuring the influence of individual features. However, these methods face challenges, including instability in explanations [3] and susceptibility to biased classifiers [41]. Pixel attribution is a method tailored for image-based models to understand model predictions by attributing importance to individual pixels [39,36,42]. However, this approach faces notable limitations, especially with ReLU activation when activation becomes capped at zero [38] and adversarial perturbations [19], as even slight alterations to an image can result in varying pixel attributions, introducing instability and inconsistency in the interpretability.

[18,7] came up with explanations from hand-picked concepts by using supervised learning. These methods use linear and non-linear classifiers on target concepts and use weights as CAVs. While these requires concepts to be picked manually, [11] uses image segmentation and clustering to curate concepts. However, due to segmentation and clustering, some information may get lost. Another downside of the method is that – it can only work with concepts that are visibly present in the images. [48] proposed improvements that address the information loss and provide a way to transform explanation back to the target model’s prediction by using Non-negative Matrix Factorization.

Individual Conditional Expectation (ICE) plots [12] and Partial Dependency Plot [10] offer local and global perspectives, respectively, on how predictions

relate to individual features. Nevertheless, they fall short of capturing complex relationships between multiple features.

We focus on the understanding of internal units of the neural network-based deep learning models. Given a deep learning model and its prediction, we ask the questions “What does the deep learning model’s internal unit represent? Are those units activated by human-understandable concepts?” Prior work has shown that internal units may indeed represent human-understandable concepts [49,5], but these approaches require semantic segmentation [46] (which is time- and compute-expensive) or explicit concept annotations [18] (which are expensive to acquire). To bypass these limitations, we use a statistical evaluation and concept activation analysis approach based on Concept Induction analysis for hypothesis generation (details in Section 3). The use of large-scale OWL background knowledge means that we draw explanations from a very large pool of explanation categories.

There has been some work using Semantic Web data to produce explanations for deep learning models [6,8], and also on using Concept Induction to provide explanations [35,29], but they focused on analysis of input-output behavior, i.e., on generating an explanation for the overall system. We focus instead on the different task of understanding internal (hidden) node activations.

The work most similar to ours in spirit, demonstrated on a similar use case, but using a completely different approach, comes from CLIP-Dissect [27] who use the CLIP pre-trained model, employing zero-shot learning to associate images with labels. Label-Free Concept Bottleneck Models [26] builds upon CLIP-Dissect and uses GPT-4 [1] for concept set generation. CLIP-Dissect, as presented, has limitations that may be non-trivial to overcome without significant changes to the approach, such as limited accuracy when predicting output labels based on concepts in the last hidden layer, not outputting a low-level concept when required (e.g., Zebra when seeing a Stripe), difficulty in transferring to other modalities or domain-specific applications (lacking an off-the-shelf concept set and the domain-specific pre-trained model). The Label-Free approach inherits the limitations of CLIP-Dissect, and appears to be somewhat self-defeating in terms of explainability, as it uses a concept derivation method which itself is *not* explainable.

In our study, we have explored the potential of Concept Induction in conjunction with large-scale background knowledge for explanation generation. This approach, aimed at understanding internal node activations, appears to be a unique contribution to the field. While other methods such as those mentioned in [27,26] have their merits, Concept Induction offers a different perspective by providing background concepts and OWL (symbolic) reasoning. It also offers a range of concept outputs, catering to different abstraction levels of concepts, and is not strictly reliant on a pre-existing, relatively small concept set or a domain-specific pre-trained concept generation model.

We have also experimented with generating relevant concepts using models trained on text and images like CLIP [30], and leveraging large language models like GPT-4 [1]. Our focus has been on quantifying the prominence of the con-

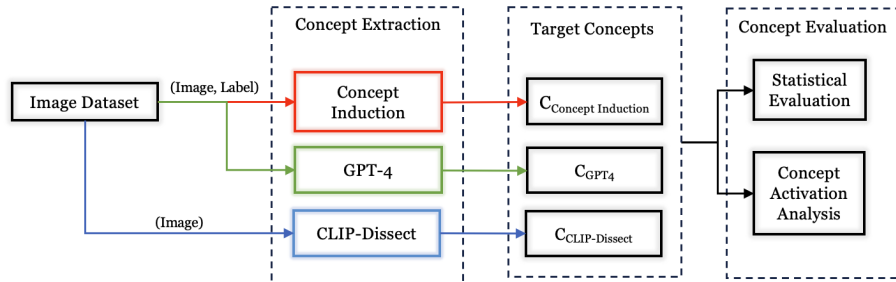


Fig. 1. An overview of the complete pipeline explored in this paper where Concept Extraction outlines the methods used to extract Target Concepts and Concept Evaluation outlines the evaluation methods.

cepts obtained from Concept Induction, CLIP, and GPT-4 within the hidden layer activation space. This has been achieved through statistical evaluation and concept activation analysis.

Our method, encompassing training, Concept Induction analysis, and evaluation analysis, is designed to be flexible and fully automatable, with the exception of the selection and provision of a suitable choice of ontology as background knowledge. It has the potential to be applied to either pre-trained models or models trained from scratch and could possibly be adapted to any neural network architecture.

3 Method

As part of the entire work, we explore and evaluate 3 concrete methods to generate high-level concepts such that those concepts potentially provide insights into hidden layer activation space. Fig. 1 is a high-level depiction of our workflow. Components are further discussed below and throughout the paper.

Preparations: Scenario and CNN Training We use a scene classification from images scenario to demonstrate our approach, drawing from the ADE20K dataset [50] which contains more than 27,000 images over 365 scenes, extensively annotated with pixel-level objects and object part labels. *The annotations are not used for CNN training*, but rather only for generating label hypotheses that we will describe in Section 3.1.

We train a classifier for the following scene categories: “bathroom,” “bedroom,” “building facade,” “conference room,” “dining room,” “highway,” “kitchen,” “living room,” “skyscraper,” and “street.” We weigh our selection toward scene categories which have the highest number of images and we deliberately include some scene categories that should have overlapping annotated

Table 1. Performance (accuracy) of different architectures on the ADE20K dataset. The system we used, based on performance, is **in bold**.

Architectures	Training acc	Validation acc
Vgg16	80.05%	46.22%
InceptionV3	89.02%	51.43%
Resnet50	35.01%	26.56%
Resnet50V2	87.60%	86.46%
Resnet101	53.97%	53.57%
Resnet152V2	94.53%	51.04%

objects – we believe this makes the hidden node activation analysis more interesting. We did not conduct any experiments on any other scene selections yet, i.e., *we did not change our scene selections based on any preliminary analyses*.

We trained a number of CNN architectures in order to use the one with highest accuracy, namely Vgg16 [40], InceptionV3 [43] and different versions of Resnet – Resnet50, Resnet50V2, Resnet101, Resnet152V2 [14,15]. Each neural network was fine-tuned with a dataset of 6,187 images (training and validation set) of size 224×224 for 30 epochs with early stopping⁴ to avoid overfitting. We used Adam as our optimization algorithm, with a categorical cross-entropy loss function and a learning rate of 0.001.

We select Resnet50V2 because it achieves the highest accuracy (see Table 1). Note that for our investigations, which focus on explainability of hidden neuron activations, achieving a very high accuracy for the scene classification task is not essential, but a reasonably high accuracy is necessary when considering models which would be useful in practice.

In the following, we will detail the different components depicted in Fig. 1. We first describe how we use Concept Induction for the generation of explanatory concepts (Section 3.1). Then we detail how we use CLIP-Dissect (Section 3.2) and GPT-4 (Section 3.3) for the same. We finally describe our two evaluation approaches (Section 3.4).

3.1 Concept Induction

Preparations: Concept Induction and Background Knowledge Base
Concept Induction [21] is based on deductive reasoning over description logics, i.e., over logics relevant to ontologies, knowledge graphs, and generally the Semantic Web field [17,16]; in particular, the W3C Standard Web Ontology Language OWL [32] is based on description logics. Concept Induction has indeed already been shown, in other scenarios, to be capable of producing labels that are meaningful for humans inspecting the data [45]. A Concept Induction system accepts three inputs: (1) a set of positive examples P , (2) a set of negative examples N , and (3) a knowledge base (or ontology) K , all expressed as description

⁴ monitor validation loss; patience 3; restore weights

logic theories, and all examples $x \in P \cup N$ occur as individuals (constants) in K . It returns description logic class expressions E such that $K \models E(p)$ for all $p \in P$ and $K \not\models E(q)$ for all $q \in N$. If no such class expressions exist, then it returns approximations for E together with a number of accuracy measures.

For scalability reasons, we use the heuristic Concept Induction system ECII [33] together with a background knowledge base that consists only of a hierarchy of approximately 2 million classes, curated from the Wikipedia concept hierarchy and presented in [34]. We use *coverage* as accuracy measure, defined as

$$\text{coverage}(E) = \frac{|Z_1| + |Z_2|}{|P \cup N|},$$

where $Z_1 = \{p \in P \mid K \models E(p)\}$ and $Z_2 = \{n \in N \mid K \not\models E(n)\}$; P is the set of all positive instances, N is the set of all negative instances, and K is the knowledge base provided to ECII as part of the input.

For the Concept Induction analysis, positive and negative example sets will contain images from ADE20K, i.e., we need to include the images in the background knowledge by linking them to the class hierarchy. For this, we use the object annotations available for the ADE20K images, but only part of the annotations for simplicity and scalability. More precisely, we only use the information that certain objects (such as windows) occur in certain images, and we do not make use of any of the richer annotations such as those related to segmentation.⁵ All objects from all images are then mapped to classes in the class hierarchy using the Levenshtein string similarity metric [22] with edit distance 0. Mapping is in fact automated using the “combine ontologies” function of ECII.

For example, `ADE_train_00001556.jpg` in the ADE20K image set has “door” listed as an object, which is mapped to the “door” concept in the Wikipedia concept hierarchy. Note that the scene information is not used for the mapping, i.e., the images themselves are not assigned to specific (scene) classes in the class hierarchy – they are connected to the hierarchy only through the objects that are shown (and annotated) in each image.

Generating Label Hypotheses The general idea for generating label hypotheses using Concept Induction is as follows: given a hidden neuron, P is a set of inputs (i.e., in this case, images) to the deep learning system that activate the neuron, and N is a set of inputs that do not activate the neuron (where P and N are the sets of positive and negative examples, respectively). As mentioned above, inputs are annotated with classes from the background knowledge for Concept Induction, but these annotations and the background knowledge

⁵ In principle, complex annotations in the form of sets of OWL axioms could of course be used, if a Concept Induction system is used that can deal with them, such as DL-Learner [21]. However DL-Learner does not quite scale to our size of background knowledge and task [35].

are not part of the input to the deep learning system. ECII generates a label hypothesis⁶ for the given neuron on inputs P , N , and the background knowledge.

We first feed 1,370 ADE20K images to our trained Resnet50V2 and retrieve the activations of the dense layer. We chose to look at the dense layer because previous studies indicate [28] that earlier layers of a CNN respond to low level features such as lines, stripes, textures, colors, while layers near the final layer respond to higher-level features such as face, box, road, etc. The higher-level features align better with the nature of our background knowledge.

The dense layer consists of 64 neurons. We chose to analyze each of the neurons separately. We are aware that activation patterns involving more than one neuron may also be informative in the sense that information may be distributed among several neurons, but the analysis of such activation patterns will be part of follow-up work.

For each neuron, we calculate the maximum activation value across all images. We then take the positive example set P to consist of all images that activate the neuron with at least 80% of the maximum activation value, and the negative example set N to consist of all images that activate the neuron with at most 20% of the maximum activation value (or do not activate it at all). The highest scoring response of running ECII on these sets, together with the background knowledge described above, is shown in Table 2 for each neuron, together with the coverage of the ECII response. For each neuron, we call its corresponding label the *target label*, e.g., neuron 0 has target label “building.” Note that some target labels consist of two concepts, e.g., “footboard, chain” for neuron 49 – this occurs if the corresponding ECII response carries two class expressions joined by a logical conjunction, i.e., in this example “footboard \sqcap chain” (as description logic expression) or $\text{footboard}(x) \wedge \text{chain}(x)$ expressed in first-order predicate logic.

We give an example, depicted in Figure 2, for neuron 1. The green and red boxed images show positive and negative examples for neuron 1. Concept Induction provides “cross_walk” as the target label. The example will be continued below.

3.2 CLIP-Dissect

CLIP-Dissect [27] is a zero-shot Explainable AI method that associates high-level concepts with individual neurons in a designated layer. Unlike traditional training-based approaches, it utilizes the pre-trained multimodal model CLIP to gauge the resemblance between a specified set of concepts and a set of test images. Using Weighted Pointwise Mutual Information, it assesses the similarities between concepts and images in the hidden layer activation space to assign a concept to a neuron. Additionally, CLIP-Dissect is label-free, meaning that it does not require the image annotations.

⁶ In fact, it generates several, ranked, but for now we use only the highest ranked one. We come back to this point further below.

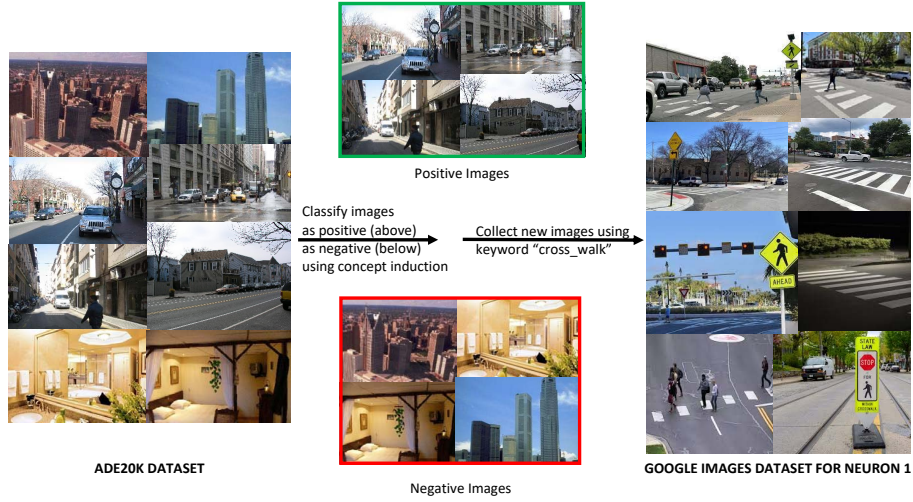


Fig. 2. Example of images that were used for generating and confirming the label hypothesis for neuron 1.

CLIP-Dissect utilizes a predefined set of the most common 20,000 English vocabulary words as concepts. To assign labels to neurons in the network under examination, we collect activations from a ResNet50v2 trained model for the ADE20K test dataset images. This results in a matrix of dimensions (Number of Images \times 64), where there are 64 hidden neuron units, and each row in the matrix represents an image through its 64 hidden neuron activation values. Combining the hidden layer representations of images with the concept set as input, CLIP-Dissect assigns a label to each neuron such that the neuron is most activated when the corresponding concept is present in the image. For the ADE20K test dataset, this process generates 22 unique concepts for the 64 neurons, with several neurons having duplicate concepts.

3.3 GPT-4

We employ a Large Language Model (LLM) using a methodology similar to our previous work [4]. Specifically, we utilize GPT-4, which represents the latest advancement in generative models and offers improved reliability, outperforming existing LLMs across various tasks [1]. These models appear capable of generating concepts essential for distinguishing between different image classes when prompted effectively [26].

For this approach, we use the same positive (P) and negative (N) example sets from Section 3.1, with some minor adjustments: For Concept Induction, the negative example set (N) comprise all images that activate the neuron with at most 20% of the maximum activation value. Due to constraints on having a large number of negative image tags as input to GPT-4, we select only one

image per class of images for each neuron to create the negative example set (N). The positive image set (P) remain unchanged, given its smaller size. All these images are sourced from the ADE20K dataset as before and are labeled with object tags present in the image.

Object tags from these images are passed into GPT-4 via the OpenAI API using prompts to generate explanations aimed at discerning the distinguishing features present in the positive set (P) that were absent in the negative set (N). These explanations were treated as concepts, and we generated a top-three list of concepts for each neuron using zero-shot prompting. For each neuron, we ran the prompt with the following parameters:

- Positive example set: object tags of all positive images (P)
- Negative example set: object tags of all negative images (N)
- Prompt question: Generate the top three classes of objects or general scenario that better represent what images in the positive set (P) have but the images in the negative set (N) do not.

We employ the most recent version of the GPT-4 model for this task, with the model’s temperature set to 0 and top_p to 1. These parameters significantly influence the output diversity of GPT-4: higher temperatures (e.g., 0.7) lead to more varied and imaginative text, whereas lower temperatures (e.g., 0.2) produce more focused and deterministic responses. Setting the temperature to 0 theoretically selects the most probable token at each step, with minor variations possible due to GPU computation nuances even under deterministic settings. In contrast to temperature sampling, which modulates randomness in token selection, top_p sampling restricts token selection to a subset (the nucleus) based on a cumulative probability mass threshold (top_p). OpenAI’s documentation advises adjusting either temperature or top_p but not both simultaneously to control model behavior effectively. For our study, setting the temperature to 0 ensured consistency and reproducibility across outputs. More detailed information regarding the experimental setup and complete prompt can be found in [4].

Although three concepts were generated for each neuron, we selected only one concept per neuron for analysis, resulting in 64 unique concepts, with several neurons having duplicate concepts.

3.4 Concept Evaluation

Confirming Label Hypotheses The three approaches described above produce label hypotheses for all investigated neurons – hypotheses that we will confirm or reject by testing the labels with new images. We use each of the target labels to search Google Images with the labels as keywords (requiring responses to be returns for *both* keywords if the label is a conjunction of classes, for Concept Induction). We call each such image a *target image* for the corresponding label or neuron. We use Imageye⁷ to automatically retrieve the images,

⁷ <https://chrome.google.com/webstore/detail/image-downloader-imageye/agionbommeaifngbhincahgmoflcikhm>

collecting up to 200 images that appear first in the Google Images search results, filtering for images in JPEG format and with a minimum size of 224x224 pixels (conforming to the size and format of ADE20K images).

For each retrieval label, we use 80% of the obtained images, reserving the remaining 20% for the statistical evaluation described later in the section. The number of images used in the hypothesis confirmation step, for each label, is given in the tables. These images are fed to the network to check (a) whether the target neuron (with the retrieval label as target label) activates, and (b) whether any other neurons activate. The Target % column of Tables 2, 3, and 4 show the percentage of the target images that activate each neuron.

Returning to our example neuron 1 in the Concept Induction case (Fig. 2), 88.710% of the images retrieved with the label “cross_walk” activate it. However, this neuron activates only for 28.923% (indicated in the Non-Target % column) of images retrieved using all other labels excluding “cross_walk.”

We define a target label for a neuron to be *confirmed* if it activates for $\geq 80\%$ of its target images regardless of how much or how often it activates for non-target images. The cut-offs for neuron activation and label hypothesis confirmation are chosen to ensure strong association and responsiveness to images retrieved under the target label, but 80% is somewhat arbitrary and could be chosen differently.

For our example neuron 1, we retrieve 233 new images with the keyword “cross_walk,” 186 of which (80%) are used in this step. 165 of these images, i.e., 88.710% activate neuron 1. Since $88.710 \geq 80$, we consider the label “cross_walk” confirmed for neuron 1.

After this step, we arrive at a list of 19 (distinct) *confirmed* labels from Concept-Induction, 5 (distinct) *confirmed* labels from CLIP-Dissect, and 14 (distinct) *confirmed* labels from GPT-4, as listed in Tables 5, 6, 7.

Statistical Evaluation After generating the confirmed labels (as above), we evaluate the node labeling using the remaining images from those retrieved from Google Images as described earlier. Results are shown in Table 5, omitting neurons that were not activated by any image, i.e., their maximum activation value was 0.

We consider each neuron-label pair (rows in Table 5, 6, 7) to be a hypothesis, e.g., for neuron 1 from Table 5, the hypothesis is that it activates more strongly for images retrieved using the keyword “cross_walk” than for images retrieved using other keywords. The corresponding null hypothesis is that activation values are *not* different. Table 5 shows the 20 hypotheses to test, corresponding to the 20 neurons with confirmed labels from method Concept Induction (recall that a double label such as neuron 16’s “mountain, bushes” is treated as one label consisting of the conjunction of the two keywords.)

Similarly, Table 6 lists the 8 hypotheses to test, corresponding to the 8 neurons with confirmed labels from method CLIP-Dissect, and Table 7 lists the 27 hypotheses to test, corresponding to the 27 neurons with confirmed labels from method GPT-4.

There is no reason to assume that activation values would follow a normal distribution, or that the preconditions of the central limit theorem would be satisfied. We therefore base our statistical assessment on the Mann-Whitney U test [24] which is a non-parametric test that does not require a normal distribution. Essentially, by comparing the ranks of the observations in the two groups, the test allows us to determine if there is a statistically significant difference in the activation percentages between the target and non-target labels.

The resulting z-scores and p-values are shown in Table 5, 6, 7 and are further discussed in Section 4. For our running example (neuron 1), we analyze the remaining 47 target images (20% of the images retrieved during the label hypothesis confirmation step). Of these, 43 (91.49%) activate the neuron with a mean and median activation of 4.17 and 4.13, respectively. Of the remaining (non-target) images in the evaluation (the sum of the image column in Table 5 minus 47), only 28.94% activate neuron 1 for a mean of 0.67 and a median of 0.00. The Mann-Whitney U test yields a z-score of -8.92 and $p < 0.00001$. The negative z-score indicates that the activation values for non-target images are indeed lower than for the target images, rejecting the null hypothesis.

It is instructive to have another look at our example neuron 1 for the Concept Induction case. The images depicted on the left in Figure 2 – target images not activating the neuron – are mostly computer-generated as opposed to photographic images as in the ADE20K dataset. The lower right image does not actually show the ground at the crosswalk, but mostly sky and only indirect evidence for a crosswalk by means of signage, which may be part of the reason why the neuron does not activate. The right-hand images are non-target images that activate the neuron. We may conjecture that other road elements, prevalent in these pictures, may have triggered the neuron. We also note that several images show bushes or plants – particularly interesting because the ECII response with the third-highest coverage score is “bushes, bush” with a coverage score of 0.993 and 48.052% of images retrieved using this label actually activate the neuron (the second response for this neuron is also “cross_walk”). It appears that Concept Induction results should be further improvable by taking additional Concept Induction returns into consideration.

Concept Activation Analysis Concept Induction is a separate process from the neural network based processes. Leveraging the strength of the background knowledge, it outputs a list of high-level concepts. A question we can ask is: how can we know if it is possible to find existence or absence of such concepts in the hidden layer activation space?

To that extent, we employ *Concept Activation* [18,7], which is a concept-based explainable AI technique which works with a *pre-defined* set of concepts. It attempts at explaining a pre-trained model by measuring the presence of *concepts* in hidden-layer activations of a given image for a particular layer. For the purpose of comparative analysis, we evaluate all candidate concepts (label hypotheses), obtained from all three methods, through Concept Activation Analysis. Note that we do not restrict this analysis to only confirmed concepts, as the Concept

Activation Analysis approach has not been developed with such a confirmation step as part of it.

For each candidate concept, a set of images are collected using Imageeye (exactly as described above) and a concept classifier (i.e. a Support Vector Machine) is trained. The dataset given to the concept classifier requires some pre-processing:

- i. The dataset for one concept classifier consists of images that exhibit the presence of the concept under description and with images where the said concept is absent. As the concept classifier will output the existence or absence of a concept, we assign the images to have labels 0 (when concept is absent) and 1 (when concept is present).

- ii. Since we are interested in finding the concepts in the hidden layer activation space, not in the image pixel space, we need to transform the image pixel values to their activation values. To achieve that, the dataset is passed across the ResNet50V2 pre-trained model as it is the network we wish to explain. The activation values of each image in the dense layer is saved. If the dense layer consists of 64 neurons, then we end up with a matrix of dimensions (no. of images \times 64).

The transformed dataset is split into train (80%) and test (20%) datasets. Thereafter, a Support Vector Machine (SVM) is trained using the train split. We have used both linear (Concept Activation Vector, CAV) and non-linear (Concept Activation Region, CAR) kernel to see which decision boundary separates the presence/absence of a concept best. Once the concept classifier is trained, a test dataset is used to see to what extent the concept classifier can classify the presence/absence of concepts in the hidden layer activation space.

We use Concept Induction, CLIP-Dissect, and GPT-4 as Concept Extraction mechanism. Thereafter we use Concept Activation analysis to measure to what extent such concepts are identifiable in the hidden layer activation space. We adopt two different kernels through CAV and CAR to train an SVM and then test the classifiers on unseen image data. Tables 8, 9, 10, and 11 represent the test accuracies for the concepts extracted by Concept Induction, CLIP-Dissect, and GPT-4. Table 12 represents the results of the Mann-Whitney U test performed over the test accuracies obtained from all 3 approaches. Table 13 shows the Mean, Median, and Standard Deviation of the test accuracies for each of the 3 approaches.

4 Results

For the given test dataset split of ADE20K, we evaluate Concept Induction, CLIP-Dissect, and GPT-4 for extracting relevant candidate concepts. Subsequently, we conduct two analyses from different perspectives:

- i. For each neuron of the dense layer, we identify the concepts that activate them the most (Statistical Evaluation).

- ii. For each concept, we measure its degree of relevance across the entire dense layer activation space (Concept Activation Analysis).

The combination of these two perspectives—a detailed examination of how each neuron unit functions and a broader view of how the dense layer operates as a whole enables us to gain a comprehensive insight into the inner workings of hidden layer computations. Regarding statistical evaluation, we rigorously assess the significance of differences in activation percentages between target and non-target labels for each confirmed label hypothesis. We compute the z-score and p-value using the non-parametric Mann-Whitney U test. Additionally, we calculate the Mean and Median for both target and non-target labels to further characterize the results. In the Concept Activation Analysis, we evaluate the effectiveness of concepts across several dimensions. Initially, we assess each concept classifier considering both linear (CAV) and non-linear (CAR) decision boundary based on the presence and absence of each concept. To validate that the concept classifier’s test accuracy is not merely coincidental, we conduct k-fold cross-validations and calculate p-values. Additionally, we compute the Mean, Median, and Standard Deviation, and perform the Mann-Whitney U test to quantify the statistical significance of the test accuracies. This comprehensive approach ensures a robust evaluation of the concepts’ performance in activating the hidden layer.

Our findings suggest that Concept Induction consistently performs well in both sets of evaluations conducted – Statistical Evaluation and Concept Activation Analysis (Section 3.4). From the statistical evaluation, it is evident that Concept Induction achieves better performance than that of CLIP-Dissect and GPT-4. In the Concept Activation Analysis, quantitative measures reveal that Concept Induction achieves comparable performance to CLIP-Dissect, with GPT-4 exhibiting the lowest performance. Conversely, the Concept Induction approach demonstrates several notable qualitative advantages over both CLIP-Dissect and GPT-4:

- CLIP-Dissect and GPT-4 are black-box models used as a concept extraction method to explain a probing network, which in this case is a CNN model, i.e., this approach to explainability is itself not readily explainable. In contrast, Concept Induction, serving as a concept extraction method, inherently offers explainability as it operates on deductive reasoning principles.
- CLIP-Dissect relies on a common English vocabulary (about 20K words) as the pool of concepts, whereas Concept Induction is supported by a meticulously constructed background knowledge (in this case with about 2M concepts), affording greater control over the definition of explanations through hierarchical relationships.
- While GPT-4/CLIP-Dissect emulate intuitive and rapid decision-making processes, Concept Induction follows a systematic and logical decision-making approach – thereby rendering our approach to be explainable by nature.

The results in Tables 5, 6, 7 show that Concept Induction analysis with large-scale background knowledge yields meaningful labels that stably explain neuron activation. Of the 20 null hypotheses from Concept Induction, 19 are rejected at $p < 0.05$, but most (all except neurons 0, 18 and 49) are rejected at much lower

p-values. Only neuron 0’s null hypothesis could not be rejected. With CLIP-Dissect, all 8 null hypotheses are rejected at $p < 0.05$, and with GPT-4, 25 out of 27 null hypotheses are rejected at $p < 0.05$, with exceptions for neurons 14 and 31. Excluding repeating concepts, Concept Induction yields **19** statistically validated hypotheses, CLIP-Dissect yields **5**, and GPT-4 yields **12**.

The Non-Target % column of Table 2 provides some insight into the results for neurons 0, 18, 49 and neurons 14, 31 from Table 4: target and non-target values for these neurons are closer to each other. Likewise, differences between target and non-target values for mean activation values and median activation values in Tables 5, 7 are smaller for these neurons. This hints at ways to improve label hypothesis generation or confirmation, and we will discuss this and other ideas for further improvement below under possible future work.

Mann-Whitney U results show that, for most neurons listed in Tables 5, 6, 7 (with $p < 0.00001$), activation values of target images are *overwhelmingly* higher than that of non-target images. The negative z-scores with high absolute values informally indicate the same, as do the mean and median values. Neurons 16 and 49 of Table 5, for which the hypotheses also hold but with $p < 0.05$ and $p < 0.01$, respectively, still exhibit statistically significant higher activation values for target than for non-target images, but not overwhelmingly so. This can also be informally seen from lower absolute values of the z-scores, and from smaller differences between the means and the medians.

For the Concept Activation Analysis evaluation, Concept Induction yields **69** unique concepts with Mean Test Accuracy of **0.9154** (CAV) and **0.9150** (CAR). CLIP-Dissect identifies **22** concepts with Mean Test Accuracy of **0.9160** (CAV) and **0.9259** (CAR). GPT-4 produces **21** concepts with Mean Test Accuracy of **0.8757** (CAV) and **0.8887** (CAR). Although, based solely on the numeric values of Mean Test Accuracy, CLIP-Dissect demonstrates a slightly superior performance compared to Concept Induction, and GPT-4 performs the least, we contend that the substantially higher number of concepts generated by Concept Induction allows CLIP-Dissect to achieve a marginally higher test accuracy. By considering the top 22 (equal to the number of concepts generated by CLIP-Dissect) test accuracies of concepts extracted by Concept Induction, the Mean Test Accuracy increases to **0.9599** (CAV) and **0.9584** (CAR). For statistical confirmation, we conduct a p-value test for K-fold cross validation, wherein all concepts in Concept Activation analysis achieve $p < 0.05$. Using a Mann-Whitney U test, we statistically ascertain that CLIP-Dissect outperforms GPT-4 in terms of CAR, and Concept Induction surpasses GPT on CAV (see Table 12).

This analysis leads us to the following conclusion: Among the three approaches we evaluate, Concept Induction demonstrates superior performance both in the quantity of high-quality concepts generated and in the relevance of these concepts within the hidden layer activation space. Furthermore, our approach possesses inherent explainability as it does not depend on any pre-trained black-box model to identify candidate concepts. However, there are undoubtedly

trade-offs involved in selecting among the three approaches, which we elaborate on in Section 5.

Based on the results obtained from the Statistical Evaluation and Concept Activation analysis, our approach introduces a novel zero-shot, model-agnostic Explainable AI technique. This technique offers insights into the hidden layer activation space by utilizing high-level, human-understandable concepts. Leveraging deductive reasoning over background knowledge, our approach inherently provides explainability while also achieving competitive performance, thus confirming our initial hypothesis.

5 Discussion

From the results of the statistical evaluation from each method, based on the percentage of target activation, if we were to categorize all confirmed concepts into three regions: high-relevance concepts (90-100%), medium-relevance concepts (80-89%), and low-relevance concepts (< 80%), Table 14 illustrates that Concept Induction produces a notably larger number of high-relevance concepts compared to CLIP-Dissect and GPT-4.

In Tables 6, 7, we present 8 and 27 statistically confirmed concepts, respectively. However, upon closer examination, it becomes evident that some concepts are duplicated across the tables. If we disregard these duplicates, Table 6 and 7 would reveal 5 and 14 confirmed concepts, respectively. Eliminating duplicate concepts is essential for accurately assessing the confirmed concepts' diversity and significance, as having duplicate concepts means we are essentially assessing the same concept multiple times. This redundancy may not add any new insights and can lead to misleading results.

From the results of Concept Activation Analysis, based on the concepts' test accuracy, if we are to bin all the concepts into 3 regions: high relevance concepts 90-100%, medium relevance concepts 80-89%, and low relevance concepts < 80%, Table 15 illustrates that Concept Induction produces a notably larger number of high-relevance concepts compared to CLIP-Dissect and GPT-4, while the latter two exhibit similar counts.

This disparity highlights Concept Induction's reliance on a rich background knowledge base, necessitating additional preprocessing but providing additional value. We argue that the candidate concept pool of 20K English vocabulary words or off-the-shelf GPT-4 do not work as one size that fits all. Concept Induction's ability to generate extensive high-relevance concepts underscores the importance of well-engineered background knowledge. That is not to say that CLIP-Dissect/GPT-4 do not provide any usefulness, there exists a trade-off of time. If the application does not require a more comprehensive set of concept-based explanations, then CLIP-Dissect/GPT-4 may appear as a useful solution especially when time is of the essence. That being said, if the application requires detailed analysis of concept-based explanations, then we argue that it is important to prepare a background knowledge and leverage Concept Induction to gain detailed insights.

Table 2. Concept Induction – The omitted neurons were not activated by any image, i.e., their maximum activation value was 0. Images: Number of images used per label. Target %: Percentage of target images activating the neuron above 80% of its maximum activation. Non-Target %: The same, but for all other images. **Bold** denotes the 20 neurons whose labels are considered confirmed.

Neuron	Obtained Label(s)	Images	Coverage	Target %	Non-Target %
0	building	164	0.997	89.024	72.328
1	cross_walk	186	0.994	88.710	28.923
3	night_table	157	0.987	90.446	56.714
6	dishcloth, toaster	106	0.999	16.038	39.078
7	toothbrush, pipage	112	0.991	75.893	59.436
8	shower_stall, cistern	136	0.995	100.000	53.186
11	river_water	157	0.995	31.847	22.309
12	baseboard, dish_rag	108	0.993	75.926	48.248
14	rocking_horse, rocker	86	0.985	54.651	47.816
16	mountain, bushes	108	0.995	87.037	24.969
17	stem	133	0.993	30.827	31.800
18	slope	139	0.983	92.086	69.919
19	wardrobe, air_conditioning	110	0.999	89.091	65.034
20	fire_hydrant	158	0.990	5.696	13.233
22	skyscraper	156	0.992	99.359	54.893
23	fire_escape	162	0.996	61.111	18.311
25	spatula, nuts	126	0.999	2.381	0.883
26	skyscraper, river	112	0.995	77.679	35.489
27	manhole, left_arm	85	0.996	35.294	26.640
28	flooring, fluorescent_tube	115	1.000	38.261	33.198
29	lid, soap_dispenser	131	0.998	99.237	78.571
30	teapot, saucepan	108	0.998	81.481	47.984
31	fire_escape	162	0.961	77.160	63.147
33	tanklid, slipper	81	0.987	41.975	30.214
34	left_foot, mouth	110	0.994	20.909	49.216
35	utensils.canister, body	111	0.999	7.207	11.223
36	tap, crapper	92	0.997	89.130	70.606
37	cistern, doorcase	101	0.999	21.782	24.147
38	letter_box, go_cart	125	0.999	28.000	31.314
39	side_rail	148	0.980	35.811	34.687
40	sculpture, side_rail	119	0.995	25.210	21.224
41	open_fireplace, coffee_table	122	0.992	88.525	16.381
42	pillar, stretcher	117	0.998	52.137	42.169
43	central_reservation	157	0.986	95.541	84.973
44	saucepan, dishrack	120	0.997	69.167	36.157
46	Casserole	157	0.999	45.223	36.394
48	road	167	0.984	100.000	73.932
49	footboard, chain	126	0.982	88.889	66.702
50	night_table	157	0.972	65.605	62.735
51	road, car	84	0.999	98.810	48.571
53	pylon, posters	104	0.985	11.538	17.332
54	skyscraper	156	0.987	98.718	70.432
56	flusher, soap_dish	212	0.997	90.094	63.552
57	shower_stall, screen_door	133	0.999	98.496	31.747
58	plank, casserole	80	0.998	3.750	3.925
59	manhole, left_arm	85	0.994	35.294	21.589
60	paper_towels, jar	87	0.999	0.000	1.246
61	ornament, saucepan	102	0.995	43.137	17.274
62	sideboard	100	0.991	21.000	29.734
63	edifice, skyscraper	178	0.999	92.135	48.761

Table 3. CLIP-Dissect – The omitted neurons were not activated by any image, i.e., their maximum activation value was 0. Images: Number of images used per label. Target %: Percentage of target images activating the neuron above 80% of its maximum activation. Non-Target %: The same, but for all other images. **Bold** denotes the 8 neurons whose labels are considered confirmed.

Neuron	Obtained Label(s)	Images	Target %	Non-target%
0	restaurants	140	55.000	59.295
1	restaurants	140	32.143	33.851
3	dresser	171	95.322	66.199
6	dining	153	7.190	50.195
7	bathroom	153	93.333	44.113
8	restaurants	140	24.286	37.957
11	highway	153	14.063	25.153
12	street	140	5.797	50.253
14	file	160	54.375	69.867
16	bathroom	171	2.000	31.722
17	furnished	169	62.130	36.390
18	dining	153	93.464	74.448
19	bathroom	149	77.333	56.471
20	buildings	107	13.725	19.610
22	road	258	51.550	46.487
23	bedroom	123	0.637	18.823
25	restaurants	140	12.857	5.044
26	restaurants	140	2.143	44.552
27	bedroom	150	2.548	27.763
28	dining	153	9.150	40.747
29	street	150	78.261	66.277
30	bed	150	29.375	36.154
31	mississauga	146	30.137	57.175
33	bathroom	150	80.667	32.955
34	microwave	102	3.922	50.240
35	roundtable	72	16.667	14.932
36	municipal	154	51.299	67.002
37	bed	160	8.125	17.670
38	bathroom	150	90.667	32.566
39	restaurants	140	26.429	39.961
40	dining	153	5.882	32.143
41	bedroom	157	64.968	34.428
42	room	156	35.897	45.206
43	highways	128	100.000	61.900
44	buildings	153	9.150	38.377
46	restaurants	140	23.571	33.269
48	bedroom	157	8.917	60.241
49	bedroom	157	95.541	55.917
50	bedroom	157	100.000	62.744
51	bedroom	157	4.459	51.951
53	kitchens	155	50.968	24.886
54	dining	153	13.725	62.857
56	bedroom	157	1.911	45.676
58	buildings	153	0.654	10.455
59	buildings	153	35.294	24.156
61	street	69	1.449	14.697
62	street	69	24.638	44.722
63	bathroom	150	16.667	47.584

Table 4. GPT-4 – The omitted neurons were not activated by any image, i.e., their maximum activation value was 0. Images: Number of images used per label. Target %: Percentage of target images activating the neuron above 80% of its maximum activation. Non-Target %: The same, but for all other images. **Bold** denotes the 27 neurons whose labels are considered confirmed.

Neuron	Obtained Label(s)	Images	Target %	Non-target%
0	Urban Landscape	176	54.545	59.078
1	Street Scene	164	92.073	29.884
3	Bedroom	165	97.576	62.967
6	Kitchen	171	86.550	51.733
7	Indoor Home Decor	177	66.102	44.793
8	Bathroom	164	98.780	47.897
11	Kitchen Scene	167	41.916	26.281
12	Indoor Home Setting	164	62.805	47.205
14	Living Room	164	82.317	65.053
16	Urban Landscape	176	73.864	28.290
17	Dining Room	159	93.711	46.339
18	Outdoor Scenery	164	92.073	73.852
19	Indoor Home Decor	177	29.379	45.571
20	Street Scene	164	68.902	14.305
22	Street Scene	164	90.244	51.273
23	Street Scene	164	81.098	19.507
25	Kitchen	171	21.637	5.628
26	Cityscape	156	73.718	28.023
27	Urban Transportation	163	66.871	30.152
28	Classroom	162	60.494	60.494
29	Bathroom	164	91.463	68.926
30	Kitchen	171	90.643	41.724
31	Urban Street Scene	163	80.864	67.201
33	Bathroom	164	74.390	37.272
34	Eyeglasses	168	65.476	45.208
35	Kitchen	171	66.667	13.224
36	Bathroom	164	95.122	61.704
37	Bathroom	164	43.902	10.487
38	Living Room	164	94.512	56.087
39	Bicycle	156	82.692	46.328
40	Living Room	164	70.122	24.156
41	Living Room	164	95.122	41.616
42	Living Room	164	48.780	46.431
43	Outdoor Urban Scene	163	91.411	57.925
44	Kitchen Scene	167	86.826	45.721
46	Kitchen Scene	167	43.114	31.155
48	Urban Street Scene	163	99.383	55.061
49	Bedroom	165	95.758	36.120
50	Living Room	164	93.902	62.756
51	Street Scene	164	98.171	43.830
53	Street Scene	164	57.317	23.575
54	Home Interior	165	26.061	63.216
56	Toilet Brush	165	94.545	35.095
57	Bathroom Interior	165	95.092	41.549
58	Kitchen Scenario	165	29.268	11.096
59	Urban Street Scene	163	87.037	26.217
60	Kitchen	171	0.585	1.691
61	Kitchen	171	60.819	11.810
62	Dining Room	159	94.969	44.128
63	Cityscape	156	95.513	47.791

Table 5. Concept Induction – Evaluation details as discussed in Section 3.4. Images: Number of images used for evaluation. # Activations: (targ(et)): Percentage of target images activating the neuron (i.e., activation at least 80% of this neuron’s activation maximum); (non-t): Same for all other images used in the evaluation. Mean/Median (targ(et)/non-t(araget)): Mean/median activation value for target and non-target images, respectively.

Neuron	Label(s)	Images	# Activations (%)		Mean		Median		z-score	p-value
			targ	non-t	targ	non-t	targ	non-t		
0	building	42	80.95	73.40	2.08	1.81	2.00	1.50	-1.28	0.0995
1	cross_walk	47	91.49	28.94	4.17	0.67	4.13	0.00	-8.92	<.00001
3	night_table	40	100.00	55.71	2.52	1.05	2.50	0.35	-6.84	<.00001
8	shower_stall, cistern	35	100.00	54.40	5.26	1.35	5.34	0.32	-8.30	<.00001
16	mountain, bushes	27	100.00	25.42	2.33	0.67	2.17	0.00	-6.72	<.00001
18	slope	35	91.43	68.85	1.59	1.37	1.44	1.00	-2.03	0.0209
19	wardrobe, air_conditioning	28	89.29	65.81	2.30	1.28	2.30	0.84	-4.00	<.00001
22	skyscraper	39	97.44	56.16	3.97	1.28	4.42	0.33	-7.74	<.00001
29	lid, soap_dispenser	33	100.00	80.47	4.38	2.14	4.15	1.74	-5.92	<.00001
30	teapot, saucepan	27	85.19	49.93	2.52	1.05	2.23	0.00	-4.28	<.00001
36	tap, crapper	23	91.30	70.78	3.24	1.75	2.82	1.29	-3.59	<.00001
41	open_fireplace, coffee_table	31	80.65	15.11	2.03	0.14	2.12	0.00	-7.15	<.00001
43	central_reservation	40	97.50	85.42	7.43	3.71	8.08	3.60	-5.94	<.00001
48	road	42	100.00	74.46	6.15	2.68	6.65	2.30	-7.78	<.00001
49	footboard, chain	32	84.38	66.41	2.63	1.67	2.30	1.17	-2.58	0.0049
51	road, car	21	100.00	47.65	5.32	1.52	5.62	0.00	-6.03	<.00001
54	skyscraper	39	100.00	71.78	4.14	1.61	4.08	1.12	-7.60	<.00001
56	flusher, soap_dish	53	92.45	64.29	3.47	1.48	3.08	0.86	-6.47	<.00001
57	shower_stall, screen_door	34	97.06	32.31	2.60	0.61	2.53	0.00	-7.55	<.00001
63	edifice, skyscraper	45	88.89	48.38	2.41	0.83	2.36	0.00	-6.73	<.00001

Table 6. CLIP-Dissect – Evaluation details as discussed in Section 3.4. Images: Number of images used for evaluation. # Activations: (targ(et)): Percentage of target images activating the neuron (i.e., activation at least 80% of this neuron’s activation maximum); (non-t): Same for all other images used in the evaluation. Mean/Median (targ(et)/non-t(araget)): Mean/median activation value for target and non-target images, respectively.

Neuron	Label(s)	Images	# Activations (%)		Mean		Median		z-score	p-value
			targ	non-t	targ	non-t	targ	non-t		
3	dresser	43	93.02	64.61	2.59	1.42	2.62	0.68	5.01	<.00001
7	bathroom	46	89.47	41.56	2.02	1.01	2.15	0.00	5.45	<.00001
18	dining	36	94.87	76.82	3.01	1.85	3.11	1.44	4.52	<.00001
33	bathroom	38	71.05	34.02	1.28	0.47	0.95	0.00	4.91	<.00001
38	bathroom	38	84.21	31.71	1.79	0.54	1.83	0.00	7.14	<.00001
43	highways	32	100.00	63.87	7.00	3.14	6.39	2.64	6.17	<.00001
49	bedroom	40	97.50	55.77	3.48	1.63	3.43	0.63	6.05	<.00001
50	bedroom	40	97.50	63.21	4.56	1.30	4.60	0.66	8.70	<.00001

Table 7. GPT-4 – Evaluation details as discussed in Section 3.4. Images: Number of images used for evaluation. # Activations: (targ(et)): Percentage of target images activating the neuron (i.e., activation at least 80% of this neuron’s activation maximum); (non-t): Same for all other images used in the evaluation. Mean/Median (targ(et)/non-t(araget)): Mean/median activation value for target and non-target images, respectively.

Neuron	Label(s)	Images	# Activations (%)		Mean		Median		z-score	p-value
			targ	non-t	targ	non-t	targ	non-t		
1	Street Scene	42	90.50	30.40	3.80	0.70	4.20	0.00	-9.62	<0.0001
3	Bedroom	42	97.60	63.40	4.70	1.20	4.90	0.70	-9.05	<0.0001
6	Kitchen	43	83.70	52.00	2.40	1.00	2.00	0.10	-5.06	<0.0001
8	Bathroom	41	100.00	44.10	4.10	1.00	4.10	0.00	-9.57	<0.0001
14	Living Room	41	78.00	67.50	1.40	1.30	1.20	0.90	-0.77	0.4413
17	Dining Room	40	97.50	45.90	2.20	0.60	2.50	0.00	-8.29	<0.0001
18	Outdoor Scenery	41	100.00	76.10	2.30	1.50	2.20	1.20	-3.96	<0.0001
22	Street Scene	42	90.50	50.10	3.00	1.40	3.30	0.00	-5.95	<0.0001
23	Street Scene	42	85.70	20.70	2.40	0.30	2.10	0.00	-10.83	<0.0001
29	Bathroom	41	90.20	68.40	2.60	1.50	2.40	1.00	-4.05	<0.0001
30	Kitchen	43	86.00	38.60	2.60	0.80	2.70	0.00	-7.22	<0.0001
31	Urban Street Scene	41	80.50	65.70	1.80	1.30	1.70	0.90	-2.4	0.164
36	Bathroom	41	100.00	61.30	3.10	1.20	2.80	0.60	-7.48	<0.0001
38	Living Room	41	92.70	54.30	2.00	1.00	2.20	0.30	-5.53	<0.0001
39	Bicycle	39	84.60	47.40	2.10	0.90	2.40	0.00	-5.64	<0.0001
41	Living Room	41	97.60	42.00	2.60	0.60	2.30	0.00	-9.31	<0.0001
43	Outdoor Urban Scene	41	92.70	56.30	4.10	2.40	4.30	1.00	-4.42	<0.0001
44	Kitchen Scene	42	81.00	43.40	2.30	1.00	2.10	0.00	-5.43	<0.0001
48	Urban Street Scene	41	100.00	52.60	4.90	2.30	4.80	0.40	-6.03	<0.0001
49	Bedroom	42	95.20	35.00	3.80	0.70	4.00	0.00	-10.31	<0.0001
50	Living Room	41	97.60	63.90	3.00	1.20	2.60	0.60	-6.78	<0.0001
51	Street Scene	42	95.20	42.90	5.70	1.50	6.10	0.00	-9.05	<0.0001
56	Toilet Brush	42	97.60	34.60	3.60	0.70	3.60	0.00	-10.48	<0.0001
57	Bathroom Interior	41	92.70	40.50	3.00	0.80	2.90	0.00	-8.35	<0.0001
59	Urban Street Scene	41	82.90	26.30	2.70	0.50	2.50	0.00	-9.06	<0.0001
62	Dining Room	40	90.00	43.90	3.30	0.80	3.70	0.00	-8.64	<0.0001
63	Cityscape	39	97.40	48.50	2.80	0.70	2.40	0.00	-8.76	<0.0001

Table 8. Concept Accuracy in Hidden Layer Activation Space of Concepts extracted using Concept Induction, where the training and test dataset is GoogleImage Dataset.

Concept Name	Method	Train Accuracy	Test Accuracy
Air Conditioner	CAR	0.8994	0.8415
Air Conditioner	CAV	0.811	0.8659
Baseboard	CAR	0.875	0.8717
Baseboard	CAV	0.8846	0.9102
Bushes	CAR	0.9150	0.9487
Bushes	CAV	0.9477	0.9743
Car	CAR	0.9464	0.9571
Car	CAV	0.925	0.9429
Coffee Table	CAR	0.9047	0.9523
Coffee Table	CAV	0.8988	0.9166
Cross Walk	CAR	0.9166	0.9468
Cross Walk	CAV	0.9247	0.9361
Dishcloth	CAR	0.9055	0.9375
Dishcloth	CAV	0.9685	0.9531
Doorcase	CAR	0.8936	0.8611
Doorcase	CAV	0.8581	0.8194
Edifice	CAR	0.9487	0.9642
Edifice	CAV	0.9548	0.9523
Fire Hydrant	CAR	0.9171	0.9625
Fire Hydrant	CAV	0.9171	0.925
Footboard	CAR	0.9268	0.9519
Footboard	CAV	0.9585	0.9423
Flusher	CAR	0.8722	0.8285
Flusher	CAV	0.9014	0.9285
Fluorescent Tube	CAR	0.9006	0.9625
Fluorescent Tube	CAV	0.9358	0.9125
Manhole	CAR	0.9349	0.8953
Manhole	CAV	0.9349	0.9302
Nuts	CAR	0.9223	0.9134
Nuts	CAV	0.9417	0.9230
Paper Towels	CAR	0.9021	0.9166
Paper Towels	CAV	0.9239	0.9166
Pipage	CAR	0.84239	0.7826
Pipage	CAV	0.7826	0.7391
Posters	CAR	0.8806	0.9230
Posters	CAV	0.8806	0.9230
Pylon	CAR	0.8397	0.8125
Pylon	CAV	0.8205	0.8375
River	CAR	0.9430	0.925
River	CAV	0.9399	0.925
Slope	CAR	0.8705	0.8714
Slope	CAV	0.9208	0.8857
Sculpture	CAR	0.8242	0.8333
Sculpture	CAV	0.8788	0.8571
Screen Door	CAR	0.9076	0.9375
Screen Door	CAV	0.9235	0.925
Spatula	CAR	0.9017	0.9431
Soap Dispenser	CAR	0.88	0.9375
Soap Dispenser	CAV	0.916	0.9531
Spatula	CAV	0.9219	0.9204
Toaster	CAR	0.927	0.9714
Toaster	CAV	0.9197	0.9736
Wardrobe	CAR	0.9375	0.95
Wardrobe	CAV	0.9188	0.9125

Concept Name	Method	Train Accuracy	Test Accuracy
Body	CAR	0.9035	0.8857
Body	CAV	0.8642	0.9
Casserole	CAR	0.9458	0.9375
Casserole	CAV	0.9808	0.975
Central Reservation	CAR	0.8694	0.9
Central Reservation	CAV	0.8917	0.9
Chain	CAR	0.9556	0.9677
Chain	CAV	0.9637	0.9677
Cistern	CAR	0.8734	0.8375
Cistern	CAV	0.8449	0.8875
Crapper	CAR	0.8516	0.8043
Crapper	CAV	0.8571	0.8695
Dish Rack	CAR	0.9375	0.9583
Dish Rack	CAV	0.9843	0.9375
Fire Escape	CAR	0.8950	0.9146
Fire Escape	CAV	0.9104	0.8902
Flooring	CAR	0.8841	0.9166
Flooring	CAV	0.8871	0.9047
Go Cart	CAR	0.9378	0.9512
Go Cart	CAV	0.9254	0.9390
Jar	CAR	0.9059	0.9333
Jar	CAV	0.9572	0.9666
Left Foot	CAR	0.8734	0.8658
Left Foot	CAV	0.8703	0.8536
Lid	CAR	0.8622	0.9047
Lid	CAV	0.8712	0.8809
Mouth	CAR	0.8963	0.9268
Mouth	CAV	0.9481	0.9512
Night Table	CAR	0.8917	0.875
Night Table	CAV	0.9235	0.8875
Open Fireplace	CAR	0.9129	0.9222
Open Fireplace	CAV	0.9101	0.9333
Ornament	CAR	0.8910	0.9375
Ornament	CAV	0.9198	0.9625
Pillar	CAR	0.8372	0.8837
Pillar	CAV	0.7732	0.8372
Plank	CAR	0.8719	0.9523
Plank	CAV	0.9146	0.9047
Road	CAR	0.9221	0.9642
Road	CAV	0.9461	0.9404
Rocking Horse	CAR	0.9173	0.9310
Rocking Horse	CAV	0.9347	0.9655
Saucepan	CAR	0.9561	0.9827
Saucepan	CAV	1	0.9827
Sideboard	CAR	0.91	0.94
Sideboard	CAV	0.965	0.92
Shower Stall	CAR	0.9409	0.9722
Shower Stall	CAV	0.9652	0.9583
Skyscraper	CAR	0.9455	0.9743
Skyscraper	CAV	0.9615	0.9743
Slipper	CAR	0.9262	0.9456
Slipper	CAV	0.9617	0.9565
Soap Dish	CAR	0.8733	0.8589
Soap Dish	CAV	0.8474	0.8589
Stem	CAR	0.8834	0.8676
Stem	CAV	0.8383	0.8382
Tap	CAR	0.8198	0.8536
Tap	CAV	0.8354	0.8902

Concept Name	Method	Train Accuracy	Test Accuracy
Building	CAR	0.9085	0.9404
Building	CAV	0.8262	0.8690
Dishrag	CAR	0.8603	0.9285
Dishrag	CAV	0.9144	0.9464
Left Arm	CAR	0.8549	0.8536
Left Arm	CAV	0.8858	0.8658
Letter Box	CAR	0.8901	0.8636
Letter Box	CAV	0.875	0.9242
Mountain	CAR	0.9426	0.95
Mountain	CAV	0.9745	0.9625
River Water	CAR	0.9554	0.9375
River Water	CAV	0.9617	0.9375
Rocker	CAR	0.8953	0.9545
Rocker	CAV	0.9457	0.8939x
Side Rail	CAR	0.9054	0.9459
Side Rail	CAV	0.8986	0.9054
Stretcher	CAR	0.89375	0.9375
Stretcher	CAV	0.9312	0.9375
Tank Lid	CAR	0.8947	0.8846
Tank Lid	CAV	0.8848	0.8717
Teapot	CAR	0.9365	0.9411
Teapot	CAV	0.9552	0.9779
Toothbrush	CAR	0.9198	0.9125
Toothbrush	CAV	0.9198	0.9
Utensils Canister	CAR	0.9262	0.925
Utensils Canister	CAV	0.9487	0.9375

Table 9. Concept Accuracy in Hidden Layer Activation Space of Combinations of Concepts extracted using Concept Induction, where the training and test dataset is GoogleImage Dataset.

Concept Name	Method	Train Accuracy	Test Accuracy
Baseboard and Dishrag	CAR	0.8694	0.8519
Baseboard and Dishrag	CAV	0.8611	0.8519
Cistern and Doorcase	CAR	0.8971	0.9038
Cistern and Doorcase	CAV	0.9207	0.9038
Dishcloth and Toaster	CAR	0.9190	0.8889
Dishcloth and Toaster	CAV	0.9231	0.9259
Edifice and Skyscraper	CAR	0.8991	0.8778
Edifice and Skyscraper	CAV	0.8733	0.8667
Flooring and Fluorescent Tube	CAR	0.8113	0.7931
Flooring and Fluorescent Tube	CAV	0.8652	0.8442
Flusher and Soap Dish	CAR	0.8649	0.8679
Flusher and Soap Dish	CAV	0.8538	0.8302
Footboard and Chain	CAR	0.9047	0.8906
Footboard and Chain	CAV	0.9246	0.8906
Left Foot and Mouth	CAR	0.9588	0.9464
Left Foot and Mouth	CAV	0.9311	0.9107
Letter Box and Go Cart	CAR	0.8800	0.8750
Letter Box and Go Cart	CAV	0.8680	0.8437
Lid and Soap Dispenser	CAR	0.9237	0.9394
Lid and Soap Dispenser	CAV	0.9722	0.9697
Manhole and Left Arm	CAR	0.8647	0.8636
Manhole and Left Arm	CAV	0.8388	0.8181
Mountain and Bushes	CAR	0.9933	0.9815
Mountain and Bushes	CAV	0.9678	0.9444
Open Fireplace and Coffee Table	CAR	0.9655	0.9838
Open Fireplace and Coffee Table	CAV	0.9508	0.9354
Ornament and Saucepan	CAR	0.8872	0.8846
Ornament and Saucepan	CAV	0.8363	0.8269
Paper Towel and Jar	CAR	0.9133	0.9090
Paper Towel and Jar	CAV	0.8719	0.8409

Concept Name	Method	Train Accuracy	Test Accuracy
Pillar and Stretcher	CAR	0.7847	0.7667
Pillar and Stretcher	CAV	0.8290	0.8000
Plank and Casserole	CAR	0.8836	0.8750
Plank and Casserole	CAV	0.8719	0.8750
Pylon and Posters	CAR	0.8605	0.8461
Pylon and Posters	CAV	0.8509	0.8269
Road and Car	CAR	0.9661	0.9524
Road and Car	CAV	0.9104	0.8909
Rocking Horse and Rocker	CAR	0.9844	0.9773
Rocking Horse and Rocker	CAV	0.9651	0.9545
Saucepan and Dishrack	CAR	0.8916	0.8870
Saucepan and Dishrack	CAV	0.9416	0.9355
Sculpture and Siderail	CAR	0.7635	0.7500
Sculpture and Siderail	CAR	0.8201	0.8167
Shower Stall and Cistern	CAR	0.9787	0.9571
Shower Stall and Cistern	CAV	0.9438	0.9571
Shower Stall and Screen Door	CAR	0.9706	0.9549
Shower Stall and Screen Door	CAV	0.9853	0.9849
Skyscaper and River	CAR	0.9596	0.9483
Skyscaper and River	CAV	0.9471	0.9310
Spatula and Nuts	CAR	0.8356	0.8125
Spatula and Nuts	CAV	0.9245	0.9063
Tap and Crapper	CAR	0.8861	0.8913
Tap and Crapper	CAV	0.8695	0.8913
Teapot and Saucepan	CAR	0.9881	0.9629
Teapot and Saucepan	CAV	0.9637	0.9444
Toothbrush and Pipeage	CAR	0.7971	0.7857
Toothbrush and Pipeage	CAV	0.8373	0.8214
Utensils Canister and Body	CAR	0.9579	0.9464
Utensils Canister and Body	CAV	0.9299	0.9107
Wardrobe and Air Conditioning	CAR	0.9309	0.9286
Wardrobe and Air Conditioning	CAV	0.9118	0.9107

Table 10. Concept Accuracy in Hidden Layer Activation Space of Concepts extracted using CLIP-Dissect.

Concept Name	Method	Train Accuracy	Test Accuracy
Bathroom	CAR	0.9700	0.9474
Bathroom	CAV	0.9400	0.9474
Bed	CAR	0.9587	0.9500
Bed	CAV	0.9437	0.9125
Bedroom	CAR	0.9167	0.9167
Bedroom	CAV	0.9137	0.9048
Buildings	CAR	0.9321	0.9230
Buildings	CAV	0.8990	0.8974
Dallas	CAR	0.9447	0.9318
Dallas	CAV	0.9750	0.9545
Dining	CAR	0.9294	0.9125
Dining	CAV	0.8907	0.9000
Dresser	CAR	0.9762	0.9625
Dresser	CAV	0.9650	0.9500
File	CAR	0.9837	0.9750
File	CAV	0.9681	0.9500
Furnished	CAR	0.8843	0.8875
Furnished	CAV	0.8762	0.8625
Highways	CAR	0.9396	0.9375
Highways	CAV	0.9679	0.9531
Interstate	CAR	0.9293	0.9268
Interstate	CAV	0.8593	0.8536
Kitchen	CAR	9848	0.9743
Kitchen	CAV	0.9590	0.9487
Legislature	CAR	0.9149	0.9000
Legislature	CAV	0.9156	0.9000
Microwave	CAR	0.9803	0.9807
Microwave	CAV	0.9873	0.9807
Mississauga	CAR	0.9041	0.9054
Mississauga	CAV	0.9467	0.9324
Municipal	CAR	0.8679	0.8461
Municipal	CAV	0.9298	0.9102
Restaurants	CAR	0.9850	0.9722
Restaurants	CAV	0.9692	0.9583
Road	CAR	0.9362	0.9250
Road	CAV	0.9387	0.9250
Room	CAR	0.8653	0.8125
Room	CAV	0.8273	0.8250
Roundtable	CAR	0.9405	0.9473
Roundtable	CAV	0.9136	0.8947
Street	CAR	0.9830	0.9722
Street	CAV	0.9347	0.9167
Valencia	CAR	0.8735	0.8625
Valencia	CAV	0.8781	0.875

Table 11. Concept Accuracy in Hidden Layer Activation Space of Concepts extracted using GPT-4.

Concept Name	Method	Train Accuracy	Test Accuracy
Bedroom	CAR	0.9851	0.9761
Bedroom	CAV	0.9660	0.9523
Bathroom Interior	CAR	0.9273	0.9146
Bathroom Interior	CAV	0.9241	0.9268
Bathroom	CAR	0.9176	0.9024
Bathroom	CAV	0.9068	0.8902
Bicycle	CAR	0.9787	0.9615
Bicycle	CAV	0.9887	0.9871
Cityscape	CAR	0.9438	0.9358
Cityscape	CAV	0.9894	0.9743
Classroom	CAR	0.8981	0.8780
Classroom	CAV	0.9012	0.8536
Dining Room	CAR	0.9256	0.9125
Dining Room	CAV	0.8942	0.8875
Eyeglasses	CAR	0.9813	0.9883
Eyeglasses	CAV	0.9883	0.9883
Home Interior	CAR	0.8515	0.8452
Home Interior	CAV	0.8363	0.8214
Indoor Home Setting	CAR	0.6713	0.6785
Indoor Home Setting	CAV	0.6890	0.6666
Indoor Home Decor	CAR	0.8428	0.8333
Indoor Home Decor	CAV	0.8418	0.8222
Kitchen Scene	CAR	0.8562	0.8571
Kitchen Scene	CAV	0.8022	0.7976
Kitchen	CAR	0.9122	0.9302
Kitchen	CAV	0.9122	0.9186
Living Room	CAR	0.8963	0.8658
Living Room	CAV	0.8658	0.8414
Outdoor Scenery	CAR	0.9135	0.9024
Outdoor Scenery	CAV	0.9054	0.9024
Outdoor Urban Scene	CAR	0.8343	0.8170
Outdoor Urban Scene	CAV	0.7650	0.7317
Street Scene	CAR	0.8819	0.8809
Street Scene	CAV	0.8568	0.8690
Toilet Brush	CAR	0.9815	0.9761
Toilet Brush	CAV	0.9727	0.9642
Urban Landscape	CAR	0.8665	0.8636
Urban Landscape	CAV	0.8922	0.8863
Urban Transportation	CAR	0.8412	0.8414
Urban Transportation	CAV	0.8251	0.8414
Urban Street Scene	CAR	0.9140	0.9024
Urban Street Scene	CAV	0.8757	0.8658

Table 12. Summary of Concept Activation Analysis results of Concept Induction, CLIP-Dissect, and GPT-4 using Mann-Whitney U test

Method	CAV		CAR	
	z-score	p-value	z-score	p-value
Concept Induction x CLIP-Dissect	0.1252	0.9004	-0.8717	0.3834
CLIP-Dissect x GPT-4	1.7494	0.0801	1.9680	0.0488
Concept Induction x GPT-4	2.1560	0.0308	1.7792	0.0751

Table 13. Summary of Concept Activation Analysis results of Concept Induction, CLIP-Dissect, and GPT-4 using Mean and Median of their respective test accuracies

Method	CAV			CAR		
	Mean	Median	Std. Deviation	Mean	Median	Std. Deviation
Concept Induction	0.9154	0.9230	0.0449	0.9150	0.9310	0.0465
CLIP-Dissect	0.9160	0.9146	0.0389	0.9259	0.9293	0.0443
GPT-4	0.8757	0.8863	0.0817	0.8887	0.9024	0.0690

In techniques like CLIP-Dissect and GPT-4, it is unclear how to meticulously craft the pool of candidate concepts. Employing a background knowledge base it is possible to make use of relationships among concepts. Concept Induction facilitates deductive reasoning utilizing this background knowledge, inherently offering transparency compared to the opaque approach of CLIP-Dissect and GPT-4 in concept extraction. This affords users flexibility in shaping the candidate concept pool, potentially serving as a valuable tool in specialized applications where a general concept pool is of limited relevance.

Our thorough analysis emphasizes the importance of exploring the selection criteria for candidates in an Explainable AI approach. While it’s crucial to investigate methods that assess the relevance of concepts in hidden layer computations within a given candidate pool, it is equally, if not more, vital to thoughtfully design this pool. Neglecting this aspect could result in overlooking crucial concepts essential for gaining insights into hidden layer computations. Our approach offers a means to integrate rich background knowledge and extract meaningful concepts from it.

One drawback of utilizing Concept Induction (and GPT-4) is its dependency on labeled image data, specifically image annotations, which serve as data points in the background knowledge. In contrast, CLIP-Dissect operates without the need for labels and can function with any provided set of images. We view this as a trade-off that must be carefully considered based on the application scenario. If the application is broad and does not demand a meticulous design of candidate concepts, then employing approaches like CLIP-Dissect can be advantageous. Conversely, for applications that are focused or specialized, CLIP-Dissect may only provide broadly relevant concepts.

While our thorough evaluation provides valuable insights into how our method performs compared to existing techniques, our focus has been primarily on assessing the effectiveness of Concept Induction within the confines of Convolutional Neural Network architecture using ADE20K Image data. Nevertheless, it is imperative to investigate its suitability across different architectures and with diverse datasets. Given the model-agnostic nature of our approach, our results suggest its potential applicability across a range of neural network architectures, datasets, and modalities. Another avenue for exploration involves examining background knowledge of varying scales and assessing its impact on extracting highly relevant concepts. While we utilized a Wiki Concept Hierarchy comprising 20 million concepts, it would be intriguing to observe the outcomes of our

approach when powered by a domain-specific Knowledge Graph in specialized domains such as Medical Diagnosis.

Table 14. Count of statistically confirmed Concepts from each method (Table 5, 6, 7) such that their percentage of target activation is binned into 3 regions based on their degree of relevance.

Method	90-100%	80-89%	<80%
Concept Induction	14	6	0
GPT-4	10	4	0
CLIP-Dissect	4	1	0

Table 15. Count of Concepts from each method such that their concept classifier’s test accuracies are binned into 3 regions based on their degree of relevance.

Method	90-100%	80-89%	<80%
Concept Induction	46	22	1
CLIP-Dissect	17	5	0
GPT-4	11	9	1

6 Conclusion

We have shown that our use of Concept Induction and large-scale ontological background knowledge leads to meaningful labeling of hidden neuron activations, confirmed by statistical analysis, which assesses the activation of neurons for both target and non-target concepts. This enables us to identify concepts that trigger the most pronounced responses from the neurons and discern meaningful patterns and associations between concepts and neuron activations, thereby enhancing the robustness and validity of our labeling methodology. Additionally, we employ Concept Activation Analysis to measure the degree of relevance of each concept across the entire dense layer activation space. This combined approach allows us to delve into the inner workings of hidden layer computations, providing a comprehensive understanding of how individual neurons function within the broader context of the dense layer’s operation. To the best of our knowledge, this approach is new, and in particular the use of large-scale background knowledge for this purpose – meaning that label categories are not restricted to a few pre-selected terms – has not been explored before. Our research has also compared the performance of other approaches such as CLIP-Dissect and GPT-4, revealing that Concept Induction outperforms these methods both quantitatively and qualitatively. However, we acknowledge that there may be some trade-offs between the methods as discussed in Section 5. Overall, our line of work aims at

comprehensive and conclusive hidden layer analysis for deep learning systems, so that, after analysis, it is possible to interpret the activations as implicit features of the input that the network has detected, thus opening up avenues to really explain the system's input-output behavior.

Acknowledgement The authors acknowledge partial funding under the National Science Foundation grants 2119753 "RII Track-2 FEC: BioWRAP (Bioplastics With Regenerative Agricultural Properties): Spray-on bioplastics with growth synchronous decomposition and water, nutrient, and agrochemical management" and 2333782 "Proto-OKN Theme 1: Safe Agricultural Products and Water Graph (SAWGraph): An OKN to Monitor and Trace PFAS and Other Contaminants in the Nation's Food and Water Systems."

References

1. Achiam, J., Adler, S., Agarwal, S., Ahmad, L., Akkaya, I., Aleman, F.L., Almeida, D., Altenschmidt, J., Altman, S., Anadkat, S., et al.: GPT-4 technical report. arXiv preprint arXiv:2303.08774 (2023)
2. Adadi, A., Berrada, M.: Peeking inside the black-box: a survey on explainable artificial intelligence (xai). *IEEE access* **6**, 52138–52160 (2018)
3. Alvarez-Melis, D., Jaakkola, T.S.: On the robustness of interpretability methods (2018), cite arxiv:1806.08049, presented at 2018 ICML Workshop on Human Interpretability in Machine Learning (WHI 2018), Stockholm, Sweden
4. Barua, A., Widmer, C., Hitzler, P.: Concept induction using LLMs: a user experiment for assessment (2024), <https://arxiv.org/abs/2404.11875>
5. Bau, D., Zhu, J.Y., Strobelt, H., Lapedriza, A., Zhou, B., Torralba, A.: Understanding the role of individual units in a deep neural network. *Proceedings of the National Academy of Sciences* **117**(48), 30071–30078 (2020)
6. Confalonieri, R., Weyde, T., Besold, T.R., del Prado Martín, F.M.: Using ontologies to enhance human understandability of global post-hoc explanations of black-box models. *Artificial Intelligence* **296**, 103471 (2021)
7. Crabbé, J., van der Schaar, M.: Concept activation regions: A generalized framework for concept-based explanations. In: Koyejo, S., Mohamed, S., Agarwal, A., Belgrave, D., Cho, K., Oh, A. (eds.) *Advances in Neural Information Processing Systems*. vol. 35, pp. 2590–2607. Curran Associates, Inc. (2022)
8. Díaz-Rodríguez, N., Lamas, A., Sanchez, J., Franchi, G., Donadello, I., Tabik, S., Filliat, D., Cruz, P., Montes, R., Herrera, F.: Explainable neural-symbolic learning (x-nesyl) methodology to fuse deep learning representations with expert knowledge graphs: The monumai cultural heritage use case. *Information Fusion* **79**, 58–83 (2022)
9. Doran, D., Schulz, S., Besold, T.R.: What does explainable AI really mean? a new conceptualization of perspectives. In: *CEUR Workshop Proceedings*. vol. 2071. CEUR (2018)
10. Friedman, J.H.: Greedy function approximation: A gradient boosting machine. *The Annals of Statistics* **29**(5), 1189 – 1232 (2001). <https://doi.org/10.1214/aos/1013203451>
11. Ghorbani, A., Wexler, J., Zou, J.Y., Kim, B.: Towards automatic concept-based explanations. In: Wallach, H., Larochelle, H., Beygelzimer, A., d'Alché-Buc, F., Fox, E., Garnett, R. (eds.) *Advances in Neural Information Processing Systems*. vol. 32. Curran Associates, Inc. (2019)
12. Goldstein, A., Kapelner, A., Bleich, J., Pitkin, E.: Peeking inside the black box: Visualizing statistical learning with plots of individual conditional expectation. *Journal of Computational and Graphical Statistics* **24**(1), 44–65 (2015). <https://doi.org/10.1080/10618600.2014.907095>
13. Gunning, D., Stefik, M., Choi, J., Miller, T., Stumpf, S., Yang, G.Z.: XAI – explainable artificial intelligence. *Science robotics* **4**(37), eaay7120 (2019)
14. He, K., Zhang, X., Ren, S., Sun, J.: Deep residual learning for image recognition. In: *Proceedings of the IEEE conference on computer vision and pattern recognition*. pp. 770–778 (2016)
15. He, K., Zhang, X., Ren, S., Sun, J.: Identity mappings in deep residual networks. In: *European conference on computer vision*. pp. 630–645. Springer (2016)
16. Hitzler, P.: A review of the semantic web field. *Commun. ACM* **64**(2), 76–83 (2021). <https://doi.org/10.1145/3397512>

17. Hitzler, P., Krötzsch, M., Rudolph, S.: Foundations of Semantic Web Technologies. Chapman and Hall/CRC Press (2010), <http://www.semantic-web-book.org/>
18. Kim, B., Wattenberg, M., Gilmer, J., Cai, C., Wexler, J., Viegas, F., Sayres, R.: Interpretability beyond feature attribution: Quantitative testing with concept activation vectors (TCAV). In: Dy, J., Krause, A. (eds.) Proceedings of the 35th International Conference on Machine Learning. Proceedings of Machine Learning Research, vol. 80, pp. 2668–2677. PMLR (10–15 Jul 2018), <https://proceedings.mlr.press/v80/kim18d.html>
19. Kindermans, P.J., Hooker, S., Adebayo, J., Alber, M., Schütt, K.T., Dähne, S., Erhan, D., Kim, B.: The (Un)Reliability of Saliency Methods, p. 267–280. Springer-Verlag, Berlin, Heidelberg (2022), https://doi.org/10.1007/978-3-030-28954-6_14
20. LeCun, Y., Bengio, Y., Hinton, G.: Deep learning. *Nature* **521**(7553), 436–444 (2015)
21. Lehmann, J., Hitzler, P.: Concept learning in description logics using refinement operators. *Mach. Learn.* **78**(1-2), 203–250 (2010). <https://doi.org/10.1007/s10994-009-5146-2>
22. Levenshtein, V.I.: On the minimal redundancy of binary error-correcting codes. *Inf. Control.* **28**(4), 268–291 (1975). [https://doi.org/10.1016/S0019-9958\(75\)90300-9](https://doi.org/10.1016/S0019-9958(75)90300-9)
23. Lundberg, S.M., Lee, S.I.: A unified approach to interpreting model predictions. In: Guyon, I., Luxburg, U.V., Bengio, S., Wallach, H., Fergus, R., Vishwanathan, S., Garnett, R. (eds.) *Advances in Neural Information Processing Systems 30*, pp. 4765–4774. Curran Associates, Inc. (2017), <http://papers.nips.cc/paper/7062-a-unified-approach-to-interpreting-model-predictions.pdf>
24. McKnight, P.E., Najab, J.: Mann-whitney u test. In: *The Corsini Encyclopedia of Psychology*. Wiley (2010)
25. Minh, D., Wang, H.X., Li, Y.F., Nguyen, T.N.: Explainable artificial intelligence: a comprehensive review. *Artificial Intelligence Review* pp. 1–66 (2022)
26. Oikarinen, T., Das, S., Nguyen, L.M., Weng, T.W.: Label-free concept bottleneck models. In: *The Eleventh International Conference on Learning Representations*. ICLR (2023), <https://openreview.net/forum?id=F1Cg47MNvBA>
27. Oikarinen, T., Weng, T.W.: CLIP-Dissect: Automatic description of neuron representations in deep vision networks. In: *International Conference on Learning Representations*. ICLR (2023), <https://openreview.net/forum?id=iPWiwWHc1V>
28. Olah, C., Mordvintsev, A., Schubert, L.: Feature visualization: How neural networks build up their understanding of images. *Distill* (November 2017). <https://doi.org/10.23915/distill.00007>
29. Procko, T., Elvira, T., Ochoa, O., Rio, N.D.: An exploration of explainable machine learning using semantic web technology. In: *2022 IEEE 16th International Conference on Semantic Computing (ICSC)*. pp. 143–146. IEEE Computer Society (jan 2022). <https://doi.org/10.1109/ICSC52841.2022.00029>
30. Radford, A., Kim, J.W., Hallacy, C., Ramesh, A., Goh, G., Agarwal, S., Sastry, G., Askell, A., Mishkin, P., Clark, J., Krueger, G., Sutskever, I.: Learning transferable visual models from natural language supervision. In: *International Conference on Machine Learning*. PMLR, vol. 139 (2021)
31. Ribeiro, M.T., Singh, S., Guestrin, C.: "Why Should I Trust You?": Explaining the Predictions of Any Classifier. In: *Proceedings of the 22nd ACM SIGKDD International Conference on Knowledge Discovery and Data Mining*. p. 1135–1144. KDD '16, Association for Computing Machinery, New York, NY, USA (2016). <https://doi.org/10.1145/2939672.2939778>, <https://doi.org/10.1145/2939672.2939778>

32. Rudolph, S., Krötzsch, M., Patel-Schneider, P., Hitzler, P., Parsia, B.: OWL 2 web ontology language primer (second edition). W3C recommendation, W3C (Dec 2012), <https://www.w3.org/TR/2012/REC-owl2-primer-20121211/>
33. Sarker, M.K., Hitzler, P.: Efficient concept induction for description logics. In: The Thirty-Third AAAI Conference on Artificial Intelligence (AAAI) The Thirty-First Innovative Applications of Artificial Intelligence Conference (IAAI), The Ninth AAAI Symposium on Educational Advances in Artificial Intelligence (EAAI). pp. 3036–3043. AAAI Press (2019). <https://doi.org/10.1609/aaai.v33i01.33013036>, <https://doi.org/10.1609/aaai.v33i01.33013036>
34. Sarker, M.K., Schwartz, J., Hitzler, P., Zhou, L., Nadella, S., Minnery, B.S., Juvina, I., Raymer, M.L., Aue, W.R.: Wikipedia knowledge graph for explainable AI. In: Villazón-Terrazas, B., Ortiz-Rodríguez, F., Tiwari, S.M., Shandilya, S.K. (eds.) Proceedings of the Knowledge Graphs and Semantic Web Second Iberoamerican Conference and First Indo-American Conference (KGSWC). Communications in Computer and Information Science, vol. 1232, pp. 72–87. Springer (2020). https://doi.org/10.1007/978-3-030-65384-2_6, https://doi.org/10.1007/978-3-030-65384-2_6
35. Sarker, M.K., Xie, N., Doran, D., Raymer, M.L., Hitzler, P.: Explaining trained neural networks with semantic web technologies: First steps. In: Besold, T.R., d’Avila Garcez, A.S., Noble, I. (eds.) Proceedings of the Twelfth International Workshop on Neural-Symbolic Learning and Reasoning (NeSy). CEUR Workshop Proceedings, vol. 2003. CEUR-WS.org (2017), https://ceur-ws.org/Vol-2003/NeSy17_paper4.pdf
36. Selvaraju, R.R., Cogswell, M., Das, A., Vedantam, R., Parikh, D., Batra, D.: Grad-cam: Visual explanations from deep networks via gradient-based localization. In: 2017 IEEE International Conference on Computer Vision (ICCV). pp. 618–626 (2017). <https://doi.org/10.1109/ICCV.2017.74>
37. Selvaraju, R.R., Das, A., Vedantam, R., Cogswell, M., Parikh, D., Batra, D.: Grad-CAM: Why did you say that? (2016), <http://arxiv.org/abs/1611.07450>
38. Shrikumar, A., Greenside, P., Kundaje, A.: Learning important features through propagating activation differences. In: Precup, D., Teh, Y.W. (eds.) Proceedings of the 34th International Conference on Machine Learning. Proceedings of Machine Learning Research, vol. 70, pp. 3145–3153. PMLR (06–11 Aug 2017), <https://proceedings.mlr.press/v70/shrikumar17a.html>
39. Simonyan, K., Vedaldi, A., Zisserman, A.: Deep inside convolutional networks: Visualising image classification models and saliency maps. CoRR **abs/1312.6034** (2013)
40. Simonyan, K., Zisserman, A.: Very deep convolutional networks for large-scale image recognition. In: 3rd International Conference on Learning Representations (ICLR 2015). Computational and Biological Learning Society (2015)
41. Slack, D., Hilgard, S., Jia, E., Singh, S., Lakkaraju, H.: Fooling lime and shap: Adversarial attacks on post hoc explanation methods. In: Proceedings of the AAAI/ACM Conference on AI, Ethics, and Society. p. 180–186. AIES ’20, Association for Computing Machinery, New York, NY, USA (2020). <https://doi.org/10.1145/3375627.3375830>, <https://doi.org/10.1145/3375627.3375830>
42. Smilkov, D., Thorat, N., Kim, B., Viégas, F.B., Wattenberg, M.: Smoothgrad: removing noise by adding noise. CoRR **abs/1706.03825** (2017)
43. Szegedy, C., Vanhoucke, V., Ioffe, S., Shlens, J., Wojna, Z.: Rethinking the inception architecture for computer vision. In: Proceedings of the IEEE conference on computer vision and pattern recognition. pp. 2818–2826 (2016)

44. Wachter, S., Mittelstadt, B.D., Russell, C.: Counterfactual explanations without opening the black box: Automated decisions and the GDPR. *CoRR* **abs/1711.00399** (2017)
45. Widmer, C., Sarker, M.K., Nadella, S., Fiechter, J., Juvina, I., Minnery, B.S., Hitzler, P., Schwartz, J., Raymer, M.L.: Towards human-compatible XAI: Explaining data differentials with concept induction over background knowledge (2022). <https://doi.org/10.48550/arXiv.2209.13710>, <https://doi.org/10.48550/arXiv.2209.13710>
46. Xiao, T., Liu, Y., Zhou, B., Jiang, Y., Sun, J.: Unified perceptual parsing for scene understanding. In: Proceedings of the European conference on computer vision (ECCV). pp. 418–434 (2018)
47. Zarlenga, M.E., Barbiero, P., Ciravegna, G., Marra, G., Giannini, F., Diligenti, M., Shams, Z., Precioso, F., Melacci, S., Weller, A., Lió, P., Jannik, M.: Concept embedding models: Beyond the accuracy-explainability trade-off. In: Advances in Neural Information Processing Systems (NeurIPS) (2022)
48. Zhang, R., Madumal, P., Miller, T., Ehinger, K.A., Rubinstein, B.I.P.: Invertible concept-based explanations for cnn models with non-negative concept activation vectors. Proceedings of the AAAI Conference on Artificial Intelligence **35**(13), 11682–11690 (May 2021). <https://doi.org/10.1609/aaai.v35i13.17389>
49. Zhou, B., Bau, D., Oliva, A., Torralba, A.: Interpreting deep visual representations via network dissection. *IEEE transactions on pattern analysis and machine intelligence* **41**(9), 2131–2145 (2018)
50. Zhou, B., Zhao, H., Puig, X., Xiao, T., Fidler, S., Barriuso, A., Torralba, A.: Semantic understanding of scenes through the ADE20K dataset. *International Journal of Computer Vision* **127**(3), 302–321 (2019)